Charged particle dynamics in a high-pressure laser ion source

P Yeates, J T Costello, E T Kennedy

Charged Particle Dynamics in a 'High Pressure' Laser Ion Source.

P. Yeates[1], J. T. Costello[1,2] and E. T. Kennedy[1,2].

[1]*National Centre for Plasma Science and Technology, Dublin City Uiversity (DCU), Glasnevin, Dublin 7, Republic of Ireland.*

[2]*School of Physics, Dublin City University (DCU), Glasnevin, Dublin 7, Republic of Ireland.*

Author: Patrick.yeates@dcu.ie, pyeates.physics@gmail.com

Abstract. Charged particle sources require beam transport techniques specific to the application for optimum operation. The complexity of techniques increases as the degree of ionization and kinetic energy of charged particles increases. The Dublin City University laser ion source (DCU - LIS) utilizes a short field region (L = 48 mm) to maximize the average charge state and peak current extracted, thus ion extraction occurs at 'high - pressure'. The presence of large space charge forces, high average plasma plume temperature and the expansion dynamics of laser generated plasmas result in significant divergence of the ion bunch upon injection into the drift tube. To facilitate efficient beam transport, and to maximize system throughput, we employ a rather unique electrostatic transport system, termed a 'continuous einzel array' (CEA). Ion electrodynamics in such a system exhibit a number of distinct features which modify the system performance and alter the expected distribution of kinetic energies (K_E), the times of flight (*TOF*) and ion bunch diameters. System scalability in regard to beam

kinetic energy is also important. In this paper the superior performance of the LIS equipped with a CEA is compared to a traditional einzel lens electrostatic beam transport system based on the usual three element and also a five element lens system.

Keywords: laser ion source, ion bunch, beam transport, simulation, SIMION.

PACS: 52.38.-r (Laser Plasma) 52.50.-Dg (Ion Sources)

Journal Title: Journal of Physics: D.

1. Introduction

Charged particle systems take many forms. Laser ion sources (LIS)[1-3], radiofrequency (RF)[4, 5] or microwave sources [6, 7], insertion devices like wigglers and undulators and related free electron laser (FEL) devices [8-10], linear particle accelerators (LINAC)[11, 12] and e - guns[13, 14] amongst others. To usefully employ the resultant electron or ion bunches, electrostatic and/or magnetic optics for transport and manipulation are often essential. Common optical elements include einzel lenses [15-17], ion energy analyzers (IEA)[18-20], quadrapoles [21], Wien [22] filters, charged grids and bending magnets.

Electrostatic optics are utilized for numerous applications such as collimation (for beam transport), focusing, energy (velocity) and charge selection, energy (velocity) compression (usually termed 'energy focusing'), space - charge force compensation and particle acceleration (or deceleration). All electrostatic optics however can be labelled filters, essentially creating differing path lengths (linear) or trajectories (radial) due to a charge or kinetic energy differential between charged particles. Einzel lenses are one of the most widely utilized electrostatic optical elements, especially in the case of laser ion sources where extensive reports on the design, analysis and simulation of einzel lenses have been published [23-28].

A primary concern for electrostatic lens designers is to ensure that the lens parameters are constant over a range of bias values. Lenses can be two element systems [29-31] however such designs do not permit a constant 'image' size to be achieved for varying bias values. Three element lenses have been studied in great detail [32-38] with regard to focusing properties, zoom range and magnification control. The above mentioned 'einzel' lens is a particular category of three element lenses, in that the central element is biased while the outer two are not (or are similarly biased). The unique property of such lenses is that the initial energy of the particle under influence is not modified [39-42] and the image position is constant. However, the magnification is not. Four element lenses can produce both a fixed image position and a constant image size [43-46]. Multiple elements are also possible, e.g., Correa *et al* in a recent publication [47] studied the concept of multiple electrostatic elements in series. Both, single 'wall', parallel plate and ring units were analytically studied and simulated for possible electrostatic trapping in lieu of magnetic bottles.

In a 'high - pressure' LIS, the divergence of the beam is very high due to the average charge state and the high ion density within the extracted plume. Combined, these two effects result in strong lateral beam expansion within the drift tube, driven by strong space - charge forces and the fast flow velocity of the primary plasma plume from which the ions are subsequently extracted. The latter originates from the explosive nature of laser plasma generation.

As the extraction voltage (V_{ext}) increases the bias required to compensate for beam divergence increases. Experimental [48-50] studies on our system indicated that the electrostatic optical system must be biased to ~ 45 - 60% of V_{ext} for efficient ion transportation and capture. The system is designed to be a compact LIS. Thus we utilize drift tubes of moderate radius (80 mm). This in turn leads to einzel cylindrical elements of diameter ~ 50 mm. Consequently, strong focusing of the rapidly expanding beam leads to

strong divergence after each focus point. LIS systems need long drift tubes (D > 1 m) to ensure a long enough time - of - flight (*TOF)* separation of differently charged ions. Such a condition requires continuous refocusing of the injected ion bunches for optimum system throughput. Experimentally, traditional three element einzel units have been found to be unsatisfactory when applied to a high - pressure LIS [48]. It becomes necessary to test experimentally the concept of a multiple element electrostatic system [47].

In this paper, we expand upon the performance of the DCU laser ion source (LIS) [48]. Specifically, we present experimental data and detailed ion electrodynamic simulations on a beam transport system that we term a 'continuous einzel array (CEA)'. Individual sections of the CEA can be biased separately, allowing the effective 'length' of this beam transport system to be varied. We have also studied the source operational performance with three element and five element lenses and compared them with the performance of the ion source with the full multiple element CEA.

2. System design

The DCU - LIS [48-50] employs a range of extraction voltages both DC (5-18 kV) and pulsed (15-50 kV). Laser intensities used to generate plasma ions range from ~10^9 - 10^{11} Wcm^{-2} *via* a Q - switched Ruby laser (τ ~35 ns, λ = 694 nm). The short field free region in our system (L = 48 mm) means that strong space - charge forces result in pronounced beam expansion and divergence upon injection into the drift tube. To minimize the beam divergence and concomitant beam loss a unique electrostatic transport system, which we term a 'continuous einzel array (CEA)' was designed and integrated into the drift tube. In combination with high extraction bias at the source, the 36 element CEA results in a number of significant gains in system performance. The specific parameters affected include the temporal duration of the collected ion bunches, the uniformity of the velocity distributions within each ion bunch and the radial properties of each charged resolved ion bunch. The total system throughput is also improved by the CEA, albeit the gain is charge dependent.

A detailed description of the electrostatic lens system design and specifications is given elsewhere [48]. The initial electrostatic transport system employed in the DCU - LIS consisted of three einzel lens units (each unit was composed of three hollow cylinders, a central element which was positively biased and two grounded cylinders, one located on either side of the central ring). These compound lens 'units' were placed at the entrance, midpoint and exit of the 2.16m long drift tube. The second and more effective system comprised the continuous einzel lens array (CEA) placed along the whole length of the drift tube. The final section of the CEA could be biased separately from the other sections of the CEA and was composed of five elements in total (two biased and three grounded).

3. Measurement and simulations

To thoroughly diagnose the effects of the CEA on the LIS performance we compared experimental data with results from detailed SIMION^{TM} simulations, focussing on three specific aspects of the system performance. Firstly, in section 3.1 we present data on the modification of the velocity distribution within the extracted Cu^+ ion bunch, at the end of the CEA. We observe a two component distribution when the CEA is biased to the high values required when the source potential, V_{ext} is high. Secondly, in section 3.2 we demonstrate strong variations in the radial focusing properties of the CEA which results in preferential focusing of ion bunches of one charge state over its neighbouring states of ionization. This is presented both experimentally and through simulations. Lastly in section 3.3, the total system throughput with the CEA, is presented, and a quantitative comparison between the CEA performance and that of the more traditional 3 and 5 - element einzel lens systems is discussed in detail.

3.1. TOF velocity group formation

The *TOF* signal recorded by a Faraday cup [48] for all extraction voltages (V_{ext}) clearly indicated a two component distribution in the current trace for charge states from Cu^{+} to Cu^{5+} when the CEA was employed to enhance beam transportation and collection. To further investigate this aspect of the extracted ion beam electrodynamics the system was simulated in SIMION^{TM}. A range of initial energies E_0 for each charge state in the simulation, corresponding to values obtained from the Langmuir probe diagnostic of the copper plasma plume within the extraction gap, were used as input to the code. The experiment [48] was performed with a laser intensity I_p ~1.13×10^{11} Wcm^{-2} and fluence F ~3.97 $kJcm^{-2}$ and the measured Maxwell - Boltzmann kinetic energy distribution of the plasma ions ranged from ~5 - 55 eV (with a peak at ~28 eV).

A series of simulations of the DCU - LIS for initial ion energies (E_0) ranging from 5 eV to 55 eV, in steps of 0.81 eV, for ion bunches composed of 500 Cu^{+} ions were performed. These energy groups were 'launched' from the planar copper target surface. Thus sixty - one different energy groups were simulated. The diameter of each monoenergetic plasma plume at creation was set to 2 mm (parallel to the simulated target surface), in accordance with the plasma plume radius upon laser pulse termination, as predicted by the MEDUSA [51, 52] laser plasma code and the Narayan and Singh [53] analytical, Eulerian 2D fluid code for our conditions. These codes utilized initial parameters which closely reproduced our experimental plasma plume [48]. The extraction bias (V_{ext}) and CEA bias values were set to those values employed experimentally. The ions were launched parallel to each other, however the Columbic repulsion factor in SIMION^{TM} was set to 5×10^{-14} C. This value was used to obtain a plasma plume which expanded through a $\pm30^{0}$ cone relative to the target normal.

For each simulated initial energy, the time of flight (*TOF*) was recorded upon arrival of the extracted ions at the end of the drift tube. The results are plotted in figure 1, for a number of initial energies (E_0). The upper inset (a) in figure 1 displays the measured kinetic

energy distribution of the plasma plume within the extraction gap obtained using a Langmuir probe [48]. The lower inset (b) displays a schematic of the simulation concept. The simulated results shown in figure 1 indicate that ions travelling along the drift tube exhibit distinct trajectories and hence a range of *TOF* values. Only ions with the highest initial energies display a relatively narrow and well defined *TOF* distribution. Particularly for lower energies, figure 1 points to a diversity of paths taken by the ions in the drift tube resulting in a broadening of the TOF distribution.

To experimentally quantify the observed two component behaviour of the extracted ion bunches, the measured *TOF* trace from the Cu^+ ion bunch was deconvoluted to generate two Gaussian functions centred at the two observed signal peaks in the Cu^+ ion bunch, for the data sets for V_{ext} = 5 - 15 kV and F = 3.97 kJcm^{-2}. Figure 2 displays the measured peak voltage for each deconvoluted velocity group plotted against the extraction voltage (V_{ext}). The upper inset (a) in figure 2 shows the *TOF* of the deconvoluted peaks for both velocity groups. The lower inset (b) displays the experimental *TOF* current trace for Cu^+ for F = 3.97 kJcm^{-2} and V_{ext} = 5 kV.

Comparing figure 1 and 2 (simulation versus experiment) we make the following observations. Ions launched close to the system axis (i.e. ion '250', bunch centre in figure 1, lower inset - b) exhibit the shortest simulated *TOF*, as expected. In comparison, ions launched at large angles relative to the system optic axis follow a more complex set of ion trajectories (main figure, figure 1). Experimentally this can be seen in figure 2 as the 'leading group' and the 'trailing group'. The leading group exhibit shorter *TOF* values (upper inset - a, figure 2) and also a moderate contribution to the total recorded Cu^+ bunch signal as V_{ext} increases. The longer *TOF* of the trailing velocity group is due to the diversity of trajectories taken by this ion group as they traverse the drift tube. Ions travelling along the most divergent trajectories experience the greatest electrostatic focusing by the CEA resulting in an extended path length and hence *TOF* from source to Faraday cup. Furthermore, as V_{ext} increases, the contribution of

the trailing edge group to the total detected signal in figure 2 grows rapidly. This result demonstrates the beneficial compensation effect in having a high source potential (V_{ext}).

To obtain a more quantitative measure of these effects, the number of simulated ions arriving within a 4 ns integration time at the Faraday cup were calculated (corresponding to the integration time on the oscilloscope). The simulation results are plotted in figure 3. The two component velocity distribution is evident with a clearly defined peak - to - peak separation. The inset in figure 3 shows the actual experimental data for F = 3.97 kJcm^{-2} for V_{ext} = 5 kV. Superimposed on this trace is a two peak Gaussian fit, identifying the *TOF* location of each peak. The simulated results display a large signal contribution from the leading edge group while the experimental results indicate a larger contribution from the trailing velocity group. This difference in the relative signal magnitudes between the leading edge and trailing edge velocity groups for the simulation versus actual results may be partly attributed to the absence of various loss mechanisms which SIMION is unable to include, e.g. ion - gas collisions. A second limitation is the simulations' approximation of the columbic inter - ion space - charge forces which broaden the beam during transport. This occurs three dimensionally and is an extremely complex process.

In a previous publication [49] the extraction efficiency (actual beam kinetic energy versus expected kinetic energy for a particular value of V_{ext}) was determined to be ~55 - 65% depending upon the laser fluence and extraction voltage used. Thus a discrepancy in the absolute *TOF* values between the simulation and experiment was expected. The difference is related to Debye shielding of the plasma bulge at the anode within the extraction gap [48, 49], leading to inefficient coupling of the electric field lines to the extracted ions. However, despite this discrepancy, the peak - to - peak separations for both data sets are in good agreement given the limitations of the simulation process. This two component temporal distribution behaviour was observed for all recorded charge resolved ion bunches (Cu^{+} - Cu^{5+}), for high extraction voltages. Thus while utilization of the CEA dramatically improves

the system throughput both in terms of the peak recorded current and the highest recorded charge state, it gives rise to a broadening of the temporal distribution of each ion bunch.

Many applications utilizing highly charged ions require good yield (ion density) per 'event', and mono - energetic ion bunches are generally preferred. For implantation studies, extracted ion bunches from the DCU - LIS, if directed at a target would implant over a range of depths. For efficient and discrete implanted layer formation, energy compression (termed energy focusing) would be required. Our experiments confirm that the contribution to the overall signal from the 'trailing velocity group' increases with V_{ext} increases (figure 2).

In contrast, the portion of the *TOF* trace (from the 'leading velocity group' saturates for $V_{ext} > 12$ kV. As V_{ext} (often termed the source potential) increases, it tends to compensate for the space - charge forces which underlie the observed beam divergence. For ions travelling almost paraxially in the drift tube, this improved beam transport process can only be applied to the extent that inter - ion repulsive forces will allow. In comparison, ions undergoing strong divergence must be strongly refocused if successful transport of this group is be achieved. Thus increased source potential must be matched by increased bias on the CEA and in combination these two actions ensure efficient transport of highly diverging ions along the drift tube.

3.2. Radial behaviour and beam focusing

The diagnostic chamber at the end of the drift tube was equipped with a range of detectors including a scanning planar probe. Orientated in the vertical plane, and facing the oncoming ion beam, the planar probe was 3 mm wide and 35 mm long. It could scan the transported ion beam radially to determine the signal response across the beam diameter. Minimum beam diameters of ~ 6 mm were recorded under optimum focusing conditions [48]. It was observed that optimum beam transport and focusing bias on the CEA for a particular ion bunch reduced the detected peak current for neighbouring charged states (an effect most

pronounced for the more highly charged ions). The extent of this preferential response to different charge states is clear from figure 4. Here the radial dependence of the detected signal trace for V_{ext} = 7 kV, F = 3.97 kJcm^{-2}, under conditions which optimized the collected Cu^{2+} ion signal via the Faraday cup, is displayed. Beam transport conditions result in a double peak structure in the radial dependence for Cu^{2+} but not for other charge states. However, these conditions did not result in optimal signals for more highly charged ions, nor did they minimize the Cu^{2+} bunch diameter at the end of the drift tube, as is clear from figure 4.

To investigate this aspect of the system performance, simulated bunches of 400 Cu^{2+} ions were launched with energies between E_0 = 5 and 55 eV, in intervals ΔE = 5 eV. The values of the source potential and einzel bias used, were determined by experiment for a) optimum throughput (T_p) and b) best focus conditions (minimum beam diameter). The radial positions of the ions upon arriving at a position in the drift tube corresponding to the position of the scanning planar probe were recorded. These results are displayed in figure 5a and 5b where the experimentally determined radial dependence of the probe peak voltage signal for Cu^{2+} ion bunch is superimposed on the results of simulations for the same charge state. The differences in the focusing properties of the CEA are clearly evident in both the experimental and simulation results. The agreement between the experimental and simulation results is better for the system when optimised for best focus. The results provide further insight into the behaviour observed earlier [48, 49] from our system regarding optimized transport. This analysis is also relevant to current density measurements, J (equal to collected current divided by beam area, $\sim I_c/A$). Many systems minimize the diameter of the aperture to their detector to prevent or minimize secondly electron emission. For beam diameters that are not matched to the detector entrance aperture, varying degrees loss of beam may result.

The challenge in balancing the desire to minimize beam diameters (and thus maximize the collected current density, J) versus charge dependent optimised system throughput (T_p) was also present in our system. Generally system throughput is defined in

terms of peak collected current of the charge state. For optimized Cu^{2+} transport and focusing conditions we noted that the Cu^{3+} collected signal decreased by ~20 - 30% and the beam diameter was not minimized. These observations are directly linked to the electrostatic lens limitations, as the bias and/or charge state changes. Such behaviours are of particular relevance to systems which rely on charge dependent *TOF* separation for accurate classification and quantification of ion yields. There is a limit on the length of a drift tube, dictated by loss mechanisms, especially vacuum constraints. Consequently, a charge resolved ion train will arrive at a detector within a window of typically a few microseconds and as it will usually require beam focusing, it will encounter the problem of preferential, charge dependent ion bunch focusing and transport. Thus the utilization of a variable circular aperture in concert with a CEA can act as a charge filter.

3.3. Beam transport

Efficient transport of extracted charged particles can be obtained at high source potential (to offset space - charge forces) and/or high ion or electron initial energies, or by employing electrostatic optics. The latter mechanism controls the flow of the extracted particles through the electric forces experienced by those particles, from multiple electric field sources/sinks, as they take diverse trajectories along the drift tube. This is especially true for an electrostatic transport system which is composed of many elements. While presenting a significant challenge, such transport systems have a number of inherent advantages. For example, laser energies and system extraction bias values have limited practical operational ranges. In comparison, a multi - component electrostatic transport system can dramatically enhance system throughput, with only minor increases in individual element bias since optical properties vary non - linearly with the applied voltages.

To investigate the main features of the transport system in the DCU - LIS, we simulated its throughput. This was achieved by launching bunches of 400 Cu^{2+} ions with a range of initial energies E_0 from 2.5 - 59 eV in increments ΔE = 2.5 eV, for an extraction

voltage V_{ext} = 7 kV. We carried through this analysis for the three different electrostatic lens systems, briefly described in the introduction. The first of these was the set of three - element compound lens 'units' placed at the entrance, midpoint and exit of the drift tube. The second system comprised the full 36 element "continuous" einzel lens array (CEA) placed along the whole length of the drift tube. The final section of the CEA could be biased separately from the other sections of the CEA and was composed of five elements in total (two biased and three grounded), which when operated alone constituted the third system examined.

Figure 6a displays the simulated percentage throughput of ions (number of ions which entered the simulated Faraday cup as a percentage of the total launched) for a source potential V_{ext} = 7 kV and a range of initial energies (E_0) of Cu^{2+} ions. The simulated electrostatic element biases were set to those utilized experimentally. In each case, the simulated ion transport systems demonstrated some losses. The CEA displayed superior beam transport for all initial energies (E_0). The full CEA and the 5 - element einzel lens displayed relatively stable increases in T_p (throughput) with E_0. This is in stark contrast to the relatively unstable T_p profile for the 3 - element transport system, reflecting the difficulty in optimizing such a system. This is related to components of each ion bunch, which cannot be efficiently transported with a simple 3 - element lens transport system, largely due to the fact that the distance between each 3 - element lens unit is greater than 0.5 m. These electrostatic 'gaps' can give rise to significant beam losses along the drift tube. As mentioned in previous work [48], bias values for the CEA were set to optimize the collected Cu^{2+} signal (as this was the largest signal). Such bias values however were not always optimum for the efficient transport of other charge states. Figure 6b displays the simulated throughput of the CEA for the charge states Cu^{+} to Cu^{3+} for E_0 = 5 - 55 eV (ΔE = 5 eV) and highlights the charge dependent behaviour of the throughput for the CEA system. Charge state selective beam transport was most pronounced when the kinetic energy of the extracted ions was increased. The differences in the efficiency of the transport systems are obvious from figure 7. Here the measured *TOF* signal for V_{ext} = 7 kV, F = 3.96 kJcm^{-2} detected at the end of the drift tube with the Faraday

cup is plotted for 1) the traditional 3 - element einzel lens units, 2) the 5 - element einzel array at the end of our drift tube (which is part of the CEA) and finally the *TOF* signal utilizing the entire CEA.

The greatest differences in the collected signals occur for the highest charge states (Cu^{3+} - Cu^{5+}) and also for the slower 'tail' regions in the *TOF* signals of each ion group. Highly charged ions experience strong transverse expansion and also possess a larger kinetic energy (K_E) gained from the extraction voltage so that they diverge most strongly. Hence, upon entering the drift tube they must be subjected to strong electrostatic focusing (which in practice occurs at numerous points along the drift tube) to ensure efficient transport of these ions from source to detector. Only the CEA can efficiently and continuously transport highly charged ions over the extended drift tube. Also notable is the changing duration and signal amplitude within a particular ion group. The superior efficiency of the CEA for all ion groups is reflected in the amplitude of the trailing edge velocity group and its contribution to the total signal at the Faraday cup which registers as a large increase in ion bunch signal duration at the tail of the pulse (figure 7, $t \sim 16$ - 21 μs region for Cu^{+}).

For *TOF* based methods of charge identification, the associated long drift tubes thus require continuous electrostatic optics if efficient beam transport, for all charge states is to be achieved. As remarked earlier, while extraction of plasma ions close to the target surface (at 'high - pressure') yields higher peak currents, higher average charge states and shorter current pulse durations, it also presents numerous challenges. These challenges are most acute for high source potentials. Table 1 shows the experimentally measured charge yields for Cu^{+} - Cu^{3+} for a range of fluences at fixed source potential V_{ext} = 5 kV, for all three tested beam transport systems. Table 2 displays the charge yields for Cu^{+} - Cu^{3+} for a range of source potentials at a fixed laser fluence (F = 3.9 $kJcm^{-2}$).

Table 1. Fluence resolved charge yield for the three beam transport systems tested experimentally. The 3 - element einzel lens system (3_{Einzel}), the 5 - element einzel lens (5_{Einzel}) and the full CEA (CEA) for Cu^{+} - Cu^{3+} at V_{ext} = 5 kV.

***F*(kJcm^{-2})**, V_{ext}**=5 kV**	**Cu^{+} (pC)**			**Cu^{2+} (pC)**			**Cu^{3+} (pC)**		
	3_{Einzel}	5_{Einzel}	CEA	3_{Einzel}	5_{Einzel}	CEA	3_{Einzel}	5_{Einzel}	CEA
910	72	184	198	216	293	419	6.15	13.2	20.6
1238	85	265	266	277	432	507	14.6	30.6	37.2
2123	112	294	337	344	489	724	25.7	66.0	76.9
3060	140	317	414	396	529	774	32.3	69.4	164
3970	172	326	392	425	544	998	34.4	71.5	236
4860	208	305	433	458	525	1051	36.4	99.5	378
5790	254	307	495	471	542	1085	42.1	118	500
6650	281	297	604	476	507	1133	47.4	83.8	604
7610	300	260	658	494	496	1165	44.8	95.5	550
8520	289	247	819	450	509	1212	25.6	184	648

Table 2. Charge yield versus V_{ext} for the three beam transport systems tested experimentally. The three unit einzel lens transport system (3_{Einzel}), the five einzel lens (5_{Einzel}) and the CEA (CEA) for Cu^{+} - Cu^{3+} at $F = 3.9$ kJcm^{-2}.

V_{ext}	Cu^{+} (pC)			Cu^{2+} (pC)			Cu^{3+} (pC)		
(F= 3.9 kJcm^{-2})	3_{Einzel}	5_{Einzel}	CEA	3_{Einzel}	5_{Einzel}	CEA	3_{Einzel}	5_{Einzel}	CEA
5	149	370	392	385	636	998	22.4	42.0	236
7	167	536	599	435	1104	1403	24.6	69.2	385
9	183	662	794	479	1680	2190	29.6	85.2	700
11	153	800	971	345	1900	2963	23.2	82.6	1282
13	102	840	1235	267	1920	3228	10.9	67.8	1540
15	90.0	725	1245	225	1810	3504	8.10	46.1	1468
17	88.0	588	924	212	1433	2620	6.20	19.8	1050

Figure 8a shows graphically the experimental charge yield versus F (for a fixed V_{ext} = 5 kV) for Cu^{2+} and figure 8b shows the Cu^{2+} charge yield versus V_{ext} (at a fixed laser flux F = 3.9 kJcm^{-2}). As stated above, the largest differences in system T_p occur at high energies i.e. high initial energy, E_0 or high source potential (V_{ext}). Figures. 8a and 8b provide interesting insight into the ion beam dynamics after injection into the drift tube. More efficient beam transport and capture as V_{ext} is increased is clearly evident in figure 8b, particularly for the CEA. This may be interpreted in terms of the 'plasma bulge' present at the anode. Debye shielding at the anode distorts the extraction field lines. Ions may be accelerated along diverging trajectories, which for high source potentials would have associated high kinetic energies. This can best be compensated for with strong electrostatic focusing throughout the ion flight times. This is only possible with the CEA. While the 5 - element einzel lens displays reasonable charge yield per kV of extraction voltage, the yield profile is no more

than half of the total achieved with the CEA. In comparison, the 3 - element lens transport system displays relatively poor system throughput and declining performance as V_{ext} is increased, this trend is evident in figure 8b. At a relatively low source potential of 5 kV, the 3 - element lens transport system can, with some success, compensate for beam expansion at the entrance to the drift tube. For 5 kV, the 5 - element array and the CEA systems are only moderately superior to the 3 - element lens system. The differences become increasingly clear as the extraction voltage increases (figure 8b). Furthermore the enhanced performance of the CEA is also evidenced in figure 8a which shows a continuously increasing T_p for increasing fluence, in clear contrast with the others.

The differences in performance are also evidenced in the increasing changes in charge yield values in Table 2 for Cu^{3+} as V_{ext} increases. For V_{ext} = 5kV the Cu^{3+} yield ratio between the three beam transport systems is 1: 1.9 : 10.5. However at V_{ext} = 13 kV this yield ratio increases to 1: 6.2 : 141. It is thus clear, that to access the benefits of a LIS configured for 'high - pressure' operation that space - charge force compensation *via* electrostatic optics must be utilized early and throughout the *TOF* of the extracted ion, as is the case for the CEA.

4. Summary

The majority of LIS systems utilize field free regions which generally exceed L ~0.5 m. This reduces the extracted plasma plume density and ensures thermalization of the ion kinetic energies [2, 3] At this point the plasma plume is a collection of neutrals and charged particles moving at uniform velocities and displaying a small velocity gradient from front to back. While this reduces the challenges of high voltage extraction and beam transport, it strongly limits the peak current and charge state which can be extracted. By minimizing the length of the field free region and consequently extracting ions at 'high - pressure' we have maximized the extracted current and charge state from the laser generated plasma. This also ensures short bunch duration, resulting in a high peak current. In doing so, a number of mechanisms dominate the extracted ion bunches dynamics. For optimum performance these

must be minimized if beam extraction, transport and collection are to be successful. It is clear from the work reported here that under such conditions electrostatic optics are crucial components of a LIS. The extent of the increase observed in figure 7 for the CEA clearly indicates the requirement for more sophisticated transport systems in a LIS when initial conditions, prior to extraction (i.e. the plasma density and charge state at the anode) deviate strongly from those normally reported in the literature. To better access the superior performance which results from extraction at 'high - pressure' utilizing a short field - free region, requires a concomitant increase in the complexity and size of secondary systems (i.e. electrostatic optics), as achieved here with the CEA system.

ACKNOWLEDGMENTS:

The authors wish to thank Enterprise Ireland for financial support in this project (grant No: SC/2003/0180).

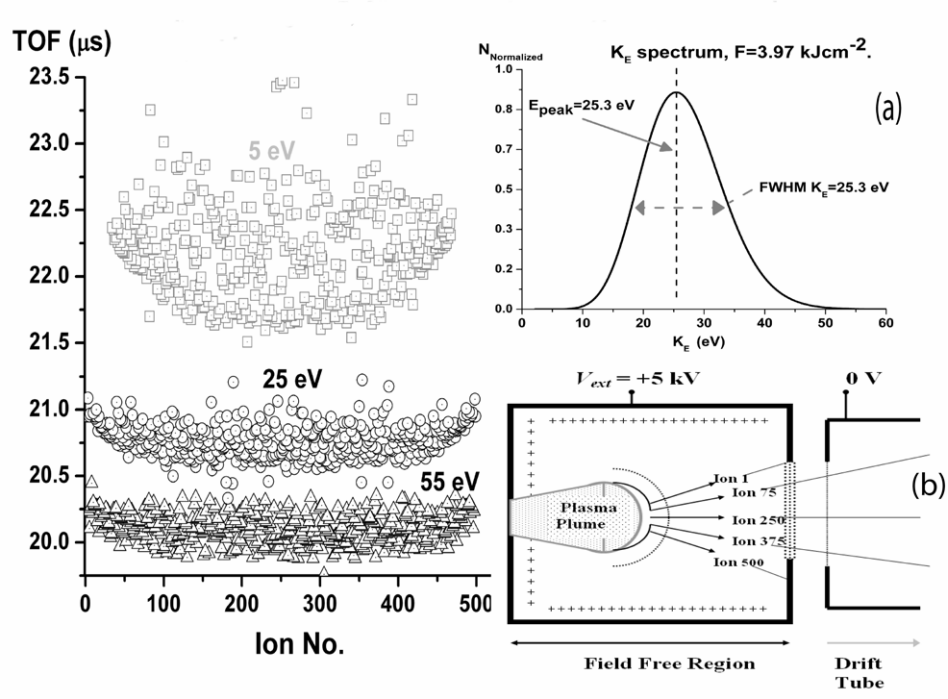

Figure 1. Simulated *TOF* times to the Faraday cup detector of separate bunches of 500 mono - energetic ions for a discrete range of initial energies (E_0 = 5, 25 and 55 eV). Inset (a): Measured kinetic energy distribution of plasma ions within the extraction gap for F = 3.97 kJcm^{-2}. Inset (b): Schematic of the simulation concept displaying the field free region and the entrance to the drift tube.

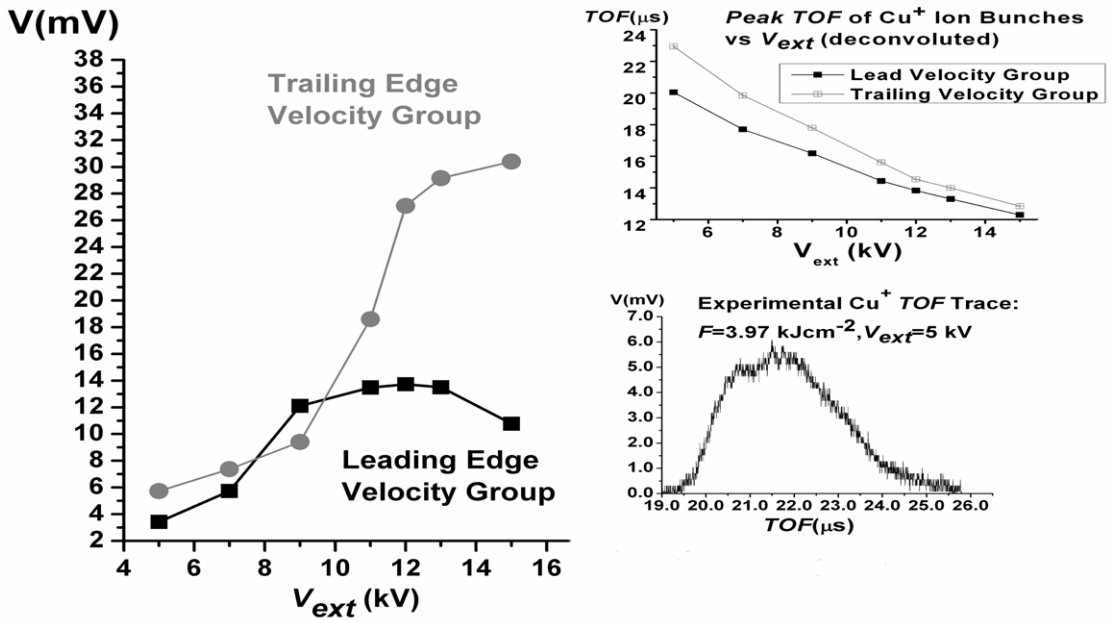

Figure 2. Measured peak voltage of the two velocity groups detected in the Cu^+ ion bunch versus the extraction voltage (V_{ext}). Time dependent traces for each velocity group were determined *via* deconvolution. Inset (a): *TOF* of the peak signal for each velocity group plotted against extraction voltage, V_{ext}. Inset (b): Experimental *TOF* trace detected *via* a Faraday cup for Cu^+ for F = 3.97 kJcm^{-2} and V_{ext} = 5 kV.

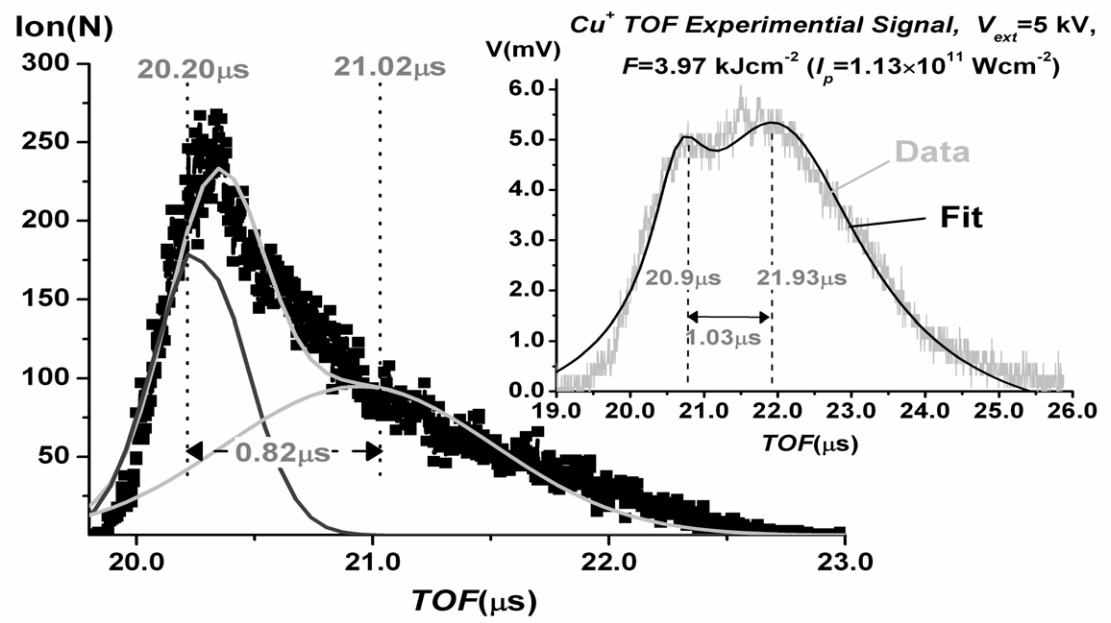

Figure 3. Simulated *TOF* times of all mono - energetic ion groups displaying a two component velocity distribution for V_{ext} = 5 kV (Time interval for each bin, Δt = 4 ns). Inset: Experimental voltage trace recorded *via* the Faraday cup at the end of the drift tube (D ~ 2.16 m), displaying the two peak Gaussian fit**.**

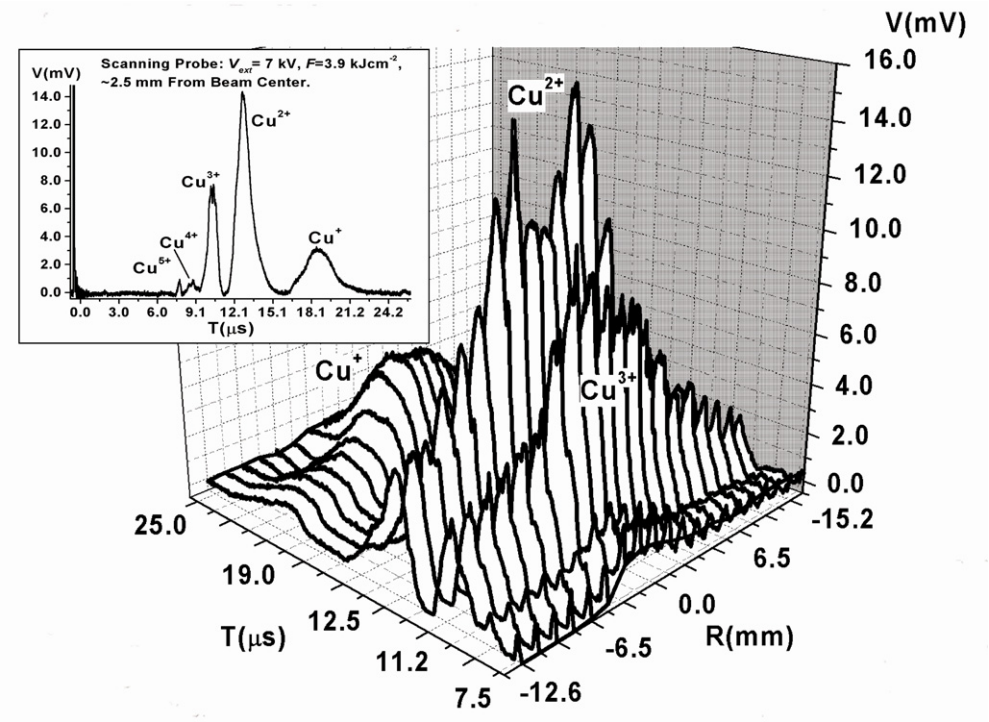

Figure 4. Experimental radial dependence of the ion beam at the end of the drift tube (V_{ext} = 7 kV, F = 3.97 kJcm^{-2}). Inset: Typical *TOF* signal from the planar probe, displaying the charged resolved ion bunches, ~ 2.5 mm radially from the system's axis.

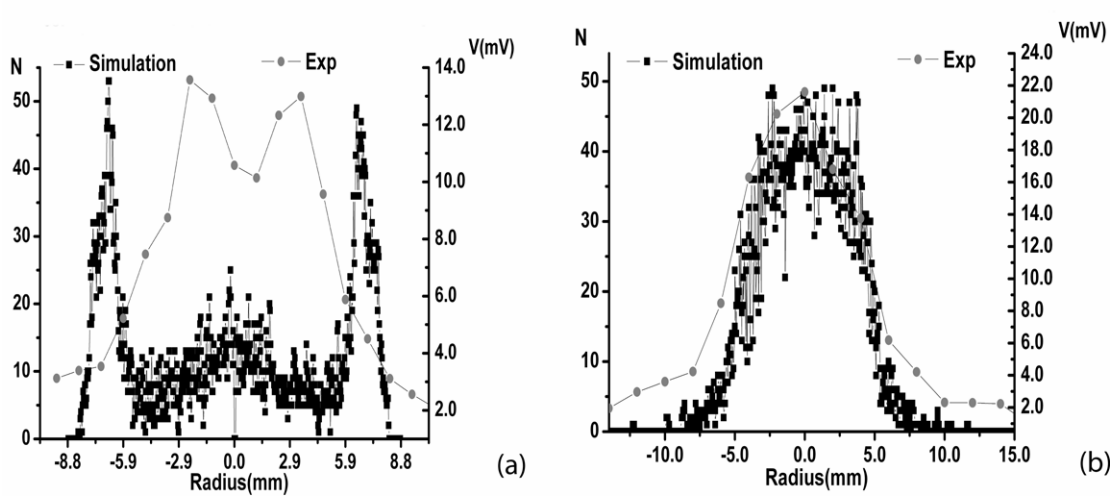

Figure 5. Cu^{2+} radially resolved scanning probe peak voltage, and simulated ion count for comparison of (a) optimum system throughput (T_p) and (b) optimum focus conditions in relation to transport and focusing performance.

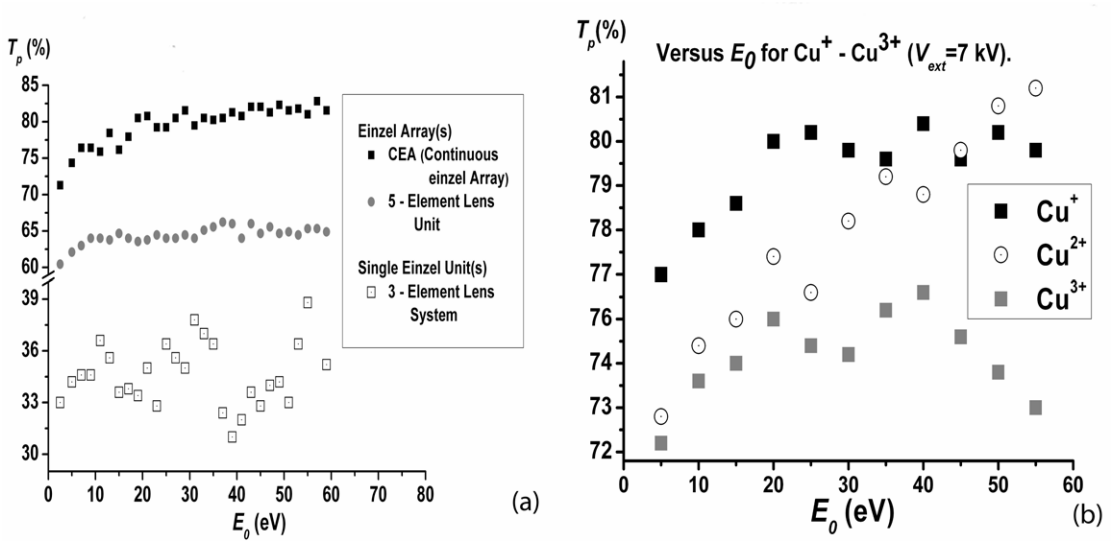

Figure 6. (a) Simulated percentage throughput (T_p) for traditional einzel 3 - element electrostatic lens transport system, the 5 - element lens array at the exit aperture of the drift tube and the CEA for V_{ext} = 7 kV and a range of initial ion energies. 400 Cu^{2+} ions for E_0 = 2.5 - 59 eV in steps of 2.5 eV were simulated for the three beam transport configurations. (b): Simulated system throughput for Cu^+ to Cu^{3+} for the CEA beam transport system versus E_0 (V_{ext} = 7 kV).

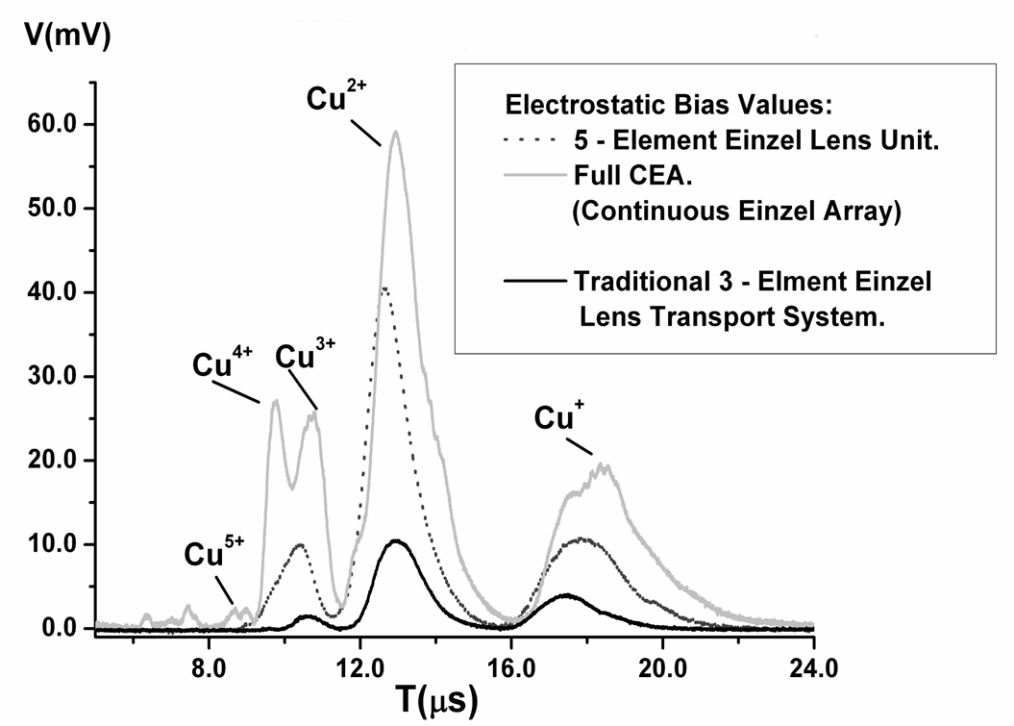

Figure 7. Experimental *TOF* signal (*via* the Faraday cup) for V_{ext} = 7 kV, F = 3.96 kJcm^{-2}, for the three electrostatic transport systems studied; the traditional 3 - element einzel lens transport system, the 5 - element lens system (at the end of the drift tube, placed in front of the Faraday cup) and the CEA.

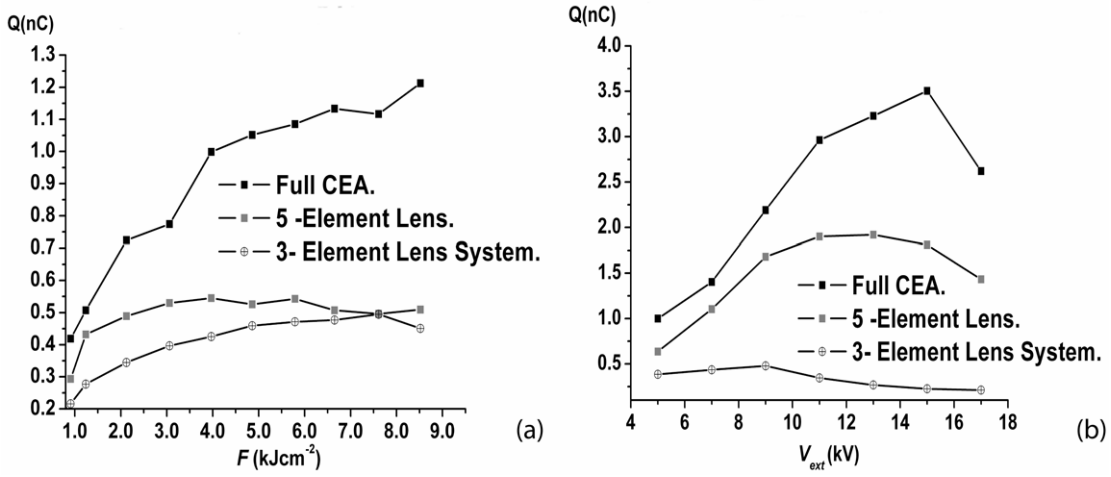

Figure 8. Fluence dependent (a) and Source potential (b) dependent, charge yields of Cu^{2+} ions for the three beam transport systems tested experimentally.

References

[1] A. Balabaev, S. Kondrashev, K. Konukov, A. Logkin, N. Mescheryakov, B. Sharkov, A. Shumshurov, S. Khomenko, K. Makarov, Rev. Sci. Instrum. Vol 73, Iss. 3, (2002) pg. 1121 - 1124.

[2] P. Fournier, G. Gregoire, H. Kugler, H. Haseroth, N. Lisi, C. Meyer, P. Ostroumov, J.- C. Schnuriger, R. Scrivens, F. Varela Rodriguez, B. H. Wolf, S. Homenko, K. Makarov, Y. Satov, A. Stepanov, S. Kondrashev, B. Sharkov, A. Shumshurov. Rev. of Sci. Instrum. Vol 71, No. 2 (2000) pg. 924 - 926.

[3] Y. Amdidouche, H. Haseroth, A. Kuttenberger, K. Langbein, J. Sellmair, B. Sharkov, O. Shamaev, T. R. Sherwood, B. Williams, Rev. Sci. Instrum. 63, 2838 (1992) pg. 2838 - 2840.

[4] K. Yamauchi, K. Takahashi, E. Yabe. Rev. Sci. Instrum. Vol. 64, Iss. 9 (1993) pg. 2434 - 2439.

[5] E. Yabe, K. Takahashi, K. Takayama. Rev. Sci. Instrum. Vol. 65, Iss. 4 (1994) pg. 1365 - 1367.

[6] M. Mozjetchkov, T. Takanashi, Y. Oka, K. Tsumori, M. Osakabe, O. Kaneko, Y. Takeiri, T. Kuroda. Rev. Sci. Instrum. Vol. 69, Iss. 2 (1998) pg. 971 - 973.

[7] Jeffrey H. Bowles, Dwight Duncan, David N. Walker, William E. Amatucci, John A. Antoniades. Rev. Sci. Instrum. Vol. 67, Iss. 2 (1996) pg. 455 - 461.

[8] J. Arthur. Rev. Sci. Instrum. Vol. 73, Iss. 3 (2002) pg. 1393 - 1395.

[9] M. W. Poole. Rev. Sci. Instrum. Vol. 63, Iss. 1 (1992) pg. 1528 - 3154.

[10] J. Arthur. Rev. Sci. Instrum. Vol. 67, Iss. 9 (1996) pg. 3345.

[11] M. Sawamura, R. Nagai, N. Kikuzawa, M. Sugimoto, N. Nishimori, E. J. Minehara. Rev. Sci. Instrum. Vol. 70, Iss. 10 (1999) pg. 3865 - 3868.

[12] T. J. Gray. Rev. Sci. Instrum. Vol. 57, Iss. 5 (1986) pg. 783.

[13] A. Kponou, E. Beebe, A. Pikin, G. Kuznetsov, M. Batazova, M. Tiunov Rev. Sci. Instrum. Vol. 69, Iss. 2 (1998) pg. 1120 - 1122.

[14] M. Merano, S. Collin, P. Renucci, M. Gatri, S. Sonderegger, A. Crottini, J. D. Ganière, B. Deveaud. Rev. Sci. Instrum. Vol. 76, Iss. 8 (2005) 085108.

[15] W. H. Aberth, R. Schnitzer, F. C. Engesser. Rev. Sci. Instrum. Vol. 45, Iss. 10 (1974) pg. 1289 - 1290.

[16] T. G. Anderson, B. G. Birdsey, S. M. Woeher, M. A. Rosenberry, T. J. Gay Rev. Sci. Instrum. Vol. 72, Iss. 7 (2001) pg. 2923 - 2925.

[17] S. K. Guharay, C. K. Allen, M. Reiser, K. Saadatmand, C. R. Chang Rev. Sci. Instrum. Vol. 65, Iss. 5 (1994) pg. 1774 - 1777.

[18] Erik A. Edelberg, Andrew Perry, Neil Benjamin, Eray S. Aydil, Rev. Sci. Instrum. Vol. 70, Iss. 6 (1999) pg. 2689 - 2698.

[19] G. Hairapetian, R. L. Stenzel. Rev. Sci. Instrum. Vol. 58, Iss. 6 (1987) pg. 2099 - 2108.

[20] M. Rhodes, J. Corbett. Rev. Sci. Instrum. Vol. 56, Iss. 5 (1985) pg. 1123 - 1125.

[21] M. Sasao, T. Kobuchi, M. Kisaki, H. Takahashi, A. Okamoto, S. Kitajima, O. Kaneko, K. Tsumori, K. Shinto, M. Wada, Rev. Sci. Instrum. Vol. 81, 02B115 (2010).

[22] E. Leal - Quiros, M. A. Prelas. Rev. Sci. Instrum. Vol. 60, Iss. 3 (1989) pg. 350 - 357.

[23] K. Saito, T. Okubo, K. Takamoto, J. Vac. Sci. Technol, A 4(2), Mar/Apr 1986.

[24] O. Sise, U. Melike, M. Dogan, Nuclear Instruments and Methods in Physics Research A 554 (2005) pg. 114 - 131.

[25] F. H. Read, A. Adams, J. R. Soto - Montiel, J. *Phys*. E: Sci. *Instrum*. **3** 1971. pg. 625 - 632.

[26] F. H. Read, A. Adams, J. *Phys*. E: Sci. *Instrum*. **5** 1972. pg. 150 - 155.

[27] F. H. Read, A. Adams, J. *Phys*. E: Sci. *Instrum*. **5** 1972. pg. 156 - 160.

[28] O. Sise, U. Melike, M. Dogan, Radiation Physics and Chemistry, 76 (2007) pg. 593 - 598.

[29] J. A. Simpson, Rev. Sci. Instrum. Vol. 35, Iss. 12 (1964) pg. 1698 - 1704.

[30] G. E. Chamberlain, Phys. Rev. 155 (1966) pg. 46.

[31] C. J. Kuyatt, J.A. Simpson, Rev. Sci. Instrum. Vol. 38, Iss. 1 (1967) pg. 103 - 111.

[32] K. Spangenberg, L.M. Field, Electron. Commun. Vol. 20, (1942) pg. 305.

[33] K. Spangenberg, L.M. Field, Electron. Commun. Vol. 21, (1943) pg. 194.

[34] P. Grivet, Electron Optics, Pergamon Press, London, 1965 (Britain).

[35] P. W. Hawkes, in: A. Septier (Ed.), Focusing of Charged Particles, Vol. 1, Academic Press, London, 1967, pp. 411 - 468.

[36] B. Paszkowski, Electron Optics, Iliffe, London, 1968 (Britain).

[37] F. H. Read, J. Phys. E 2 (1969) pg. 165.

[38] O. Klemperer, M.E. Barnett, Electron Optics, Third ed, Cambridge University Press, Cambridge, 1971 (United Kingdom).

[39] A. B. El - Kareh, M.A. Sturans, J. Appl. Phys. Vol. 42, Iss. 5 (1971) pg. 1870 - 1876.

[40] A. B. El - Kareh, M.A. Sturans, J. Appl. Phys. Vol. 42, Iss. 12 (1971) pg. 4902 - 4907.

[41] F. H. Read, J. Phys. E 2 (1969) pg. 679.

[42] G.N.H. Riddle, J. Vac. Sci. Technol. 15 (3) (1978) pg. 857.

[43] A. Chutjian, J. Chem. Phys. 61 (10) (1974) pg. 4279.

[44] J. N. H. Brunt, F. H. Read, G.C. King, J. Phys. E 10 (1977) pg. 134.

[45] M. V. Kurepa, M. D. Tasic, J.M. Kurepa, J. Phys. E 7 (1974) pg. 940.

[45] J. Fink, E. Kisker, Rev. Sci. Instrum. Vol. 51, Iss. 7 (1980) pg. 918 - 920.

[46] E. Kisker, Rev. Sci. Instrum. Vol. 53, Iss. 1 (1982) pg. 114 - 116.

[47] J. R. Correa, C. A. Ordonez, D. L. Weathers, Nuclear Instruments and Methods in Physics Research B 241 (2005) pg. 909 - 912.

[48] P. Yeates, J. T. Costello, E. T. Kennedy. Rev. Sci. Instrum. Vol. 81, Iss. 4 (2010) pg. 3305 - 3318.

[49] P. Yeates, J. T. Costello, E. T. Kennedy. Plasma Sources Sci. Technol. 19 (2010) 065007.

[50] P. Yeates, J. T. Costello, E. T. Kennedy, Physics of Plasmas, Vol 17, Iss. 12 (2010) pp. 10 (*In Press*).

[51] Christiansen, J. P. Ashby, D. E. T. F. Roberts, K. V. Computer Physics Communications, Vol 7, Issue 5, p. 271-287.

[52] Djaoui A, Rose SJ. Calculation of the time - dependent excitation and ionization in laser - produced plasma. J. Phys B: At Mol Opt Phys 1992;25:2745 - 62.

[53] R. K. Singh, J. Narayan, Phys. Rev. B 41, pg. 8843 - 8859 (1990).